93　　9　　23

行政院國家科學委員會補助專題研究計畫成果報告

※※※※※※※※※※※※※※※※※※※※※※※※

建立轉錄調節序列表現及蛋白質體系統於治療嚴重

急性呼吸道症候群之中草藥有效成分篩選

※※※※※※※※※※※※※※※※※※※※※※※※

計畫類別：■個別型計畫　　□整合型計畫

計畫編號：NSC92-2751-B-039-009-Y

執行期間：92 年 7 月 1 日至 93 年 6 月 30 日

計畫主持人：蔡長海

共同主持人：蔡輔仁　林振文　賴建成　陳建仲

執行單位：中國醫藥大學

中 華 民 國　　93 年　9 月　23 日

行政院國家科學委員會專題研究計畫成果報告

主持人：　　蔡長海　中國醫藥大學醫學系

共同主持人：蔡輔仁　中國醫藥大學附設醫院醫研部

　　　　　　林振文　中國醫藥大學醫學檢驗生物技術系

　　　　　　賴建成　中國醫藥大學附設醫院醫研部

　　　　　　陳建仲　中國醫藥大學中醫系

Abstract

Part I: **Characterization of *Trans*- and *Cis*-Cleavage Activity of the SARS Coronavirus 3CL^{pro} Protease: Basis for the in Vitro Screening of anti-SARS Drugs (This part has published in FEBS Letters 2004 Sep 10;574(1-3):131-7)**

Severe acute respiratory syndrome (SARS) has been globally reported. A novel coronavirus, SARS-coronavirus (SARS-CoV) was identified as the etiological agent of the disease. SARS-CoV 3C-like protease (3CL^{pro}) mediates the proteolytic processing of replicase polypeptides 1a and 1ab into functional proteins, playing an important role in viral replication. In this study, we demonstrated the expression of the SARS-CoV 3CL^{pro} in *E. coli* and Vero cells, and then characterized the in vitro *trans*-cleavage and the cell-based *cis*-cleavage by the 3CL^{pro}. Mutational analysis of the 3CL^{pro} demonstrated the importance of His41, Cys145, and Glu166 in the substrate-binding subsite S1 for keeping the proteolytic activity. In addition, alanine substitution of the cleavage substrates indicated that Gln-$_{P1}$ in the substrates mainly determined the cleavage efficiency. Therefore, this study not only established the quantifiable and reliable assay for the in vitro and cell-based measurement of the

3CL^{pro} activity, but also characterized the molecular interaction of the SARS-CoV 3CL^{pro} with the substrates.   The results will be useful for the rational development of the anti-SARS drugs.

Key words:
SARS-coronavirus; 3C-like protease; *trans-* and *cis-*cleavage; substrate specificity

Part II: Studies on the Anti- SARS Coronavirus 3C-like Protease Effect of the *Isatis Indigotica* Root (This part has been submitted to FEBS Letters)

The 3C-like protease (3CL^{pro}) of SARS-coronavirus mediates the proteolytic processing of replicase polypeptides 1a and 1ab into functional proteins, becoming an important target for the drug development.   In this study, we demonstrated the anti-3CL^{pro} effect of the *Isatis Indigotica* root extract using the in vitro *trans-*cleavage and in vivo *cis-*cleavage assays.   The extract of *Isatis Indigotica* Root showed a dose-dependent manner of the anti-3CL^{pro} effect with the 50% inhibitory concentration (IC$_{50}$) of 80.3 ± 4.2 µg/ml for the in vitro trans-cleavage assay and 191.6 ± 8.2 µg/ml for the cell-based *cis-*cleavage assay.   Of compounds from *Isatis Indigotica* Root, indigo, sinigrin and beta-sitosterol also had the anti-3CL^{pro} effect in a significant dose-dependent manner.   The results indicated the therapeutic value of the *Isatis Indigotica* root against SARS.   The study provides a rational approach to develop the combination of Chinese herbs with the potential anti-SARS compounds for the treatment of the SARS patients.

Key words: SARS-coronavirus; 3C-like protease; *Isatis Indigotica* Root

Part Ⅰ: **Characterization of *Trans*- and *Cis*-Cleavage Activity of the SARS Coronavirus 3CL^pro Protease: Basis for the in Vitro Screening of anti-SARS Drugs**

1. Introduction

Severe acute respiratory syndrome (SARS) with high fever, malaise, headache, dry cough and a progress of generalized, interstitial infiltrates in the lung has recently reported over 32 countries around the world, including Taiwan, China, Hong Kong, Vietnam, and Canada [1-4]. SARS was rapidly transmitted through aerosols, causing 8,447 reported cases with 811 deaths worldwide in a short period from February to June, 2003 [5-7]. For successful control of the SARS outbreak, developing effective therapies and vaccines becomes medically important efforts.

A novel coronavirus, SARS-coronavirus (SARS-CoV) was identified as the etiological agent of the disease [1-4]. SARS-CoV particles contain a single positive-stranded RNA genome that is approximately 30 kb in length and has a 5' cap structure and 3' polyA tract [8-10]. The SARS-CoV genome encodes for replicase, spike, envelope, membrane, and nucleocapsid. The replicase gene encodes two large overlapping polypeptides (replicase 1a and 1ab, ~ 450kD and ~750kD, respectively), including 3C-like protease (3CL^pro), RNA-dependent RNA polymerase, and RNA helicase for viral replication and transcription [11]. The SARS-CoV 3CL^pro mediates the proteolytic processing of replicase polypeptides 1a and 1ab into functional proteins, playing an important role in viral replication. Eleven cleavage sites of the 3CL^pro on the viral polyprotein have been mapped using the computer prediction based the substrate conservation among coronavirus main proteases [12], being confirmed by the in vitro *trans*-cleavage of 11 substrate peptides [13]. Therefore, the SARS-CoV 3CL^pro becomes an attractive target for developing effective drugs against SARS.

In this study, we characterized the in vitro *tans*-cleavage and the cell-based *cis*-cleavage with the SARS-CoV 3CL^pro (Fig. 1A and 1B). For the *trans*-cleavage assay, the functional 3CL^pro and three mutants at the substrate-binding sites were used to test their proteolytic activity with the cleavage substrate-I (TVRLQAGNAT) fused at the N-terminus of the SARS-CoV non-structure protein 7 (nsp7). For the *cis*-cleavage assay, the in-frame construction of the 3CL^pro, the substrate-II (SAVLQSGFRK), and the luciferase was transfected into the Vero cells. In addition, the mutations at the substrate conserved residues Leu and Gln were performed for the examination of the substrate specificity. In this study, the in vitro *tans*-cleavage and

cell-based *cis*-cleavage activities of the SARS-CoV 3CL^{pro} had been determined using the quantitative methods of an Enzyme-Linked Immunosorbent Assay (ELISA) and a luciferase assay, which will be useful for large-scale screening of inhibitors against SARS.

2. Materials and Methods

2.1. Construction, expression, and purification of SARS-CoV 3CL^{pro}

The 3CL^{pro} gene located within the nucleotides 9985 to 10902 of the SARS-CoV TW1 strain genome (GenBank accession No. AY291451) [14] was amplified using the reverse-transcriptase polymerase chain reaction (RT-PCR) with specific primers 5'-CCCGGATCCAGTGGTTTTAGGAAAATGGCATTC-3' and 5'-GGTGCTCGAGTTGGAAGGTAACACCAGAGCATTG-3'.   The forward primer mentioned above contained an *Eco*RI restriction site, and the reverse primers included an *Xho*I restriction site.   Each RT-PCR product was digested with *Eco*RI and *Xho*I, and then ligated into the *Eco*RI/*Xho*I cleavage sites of the pET24a vector (Novagen) and expressed as a histidine tag fusion protein.   The *E. coli* strain BL21(DE3) was transformed with the resulting plasmid, pET24a-3CL^{pro}, then cultured in LB medium in the presence of 100 μg of kanamycin per ml at 37℃. Once the cultures reached an absorbance at 600nm of 0.5 to 0.6, they were induced by the addition of 4 mM isopropyl-β-D-thiogalactopyranoside (IPTG) for 4 h at 22℃. Finally, the bacteria were harvested by centrifugation at 10000 rpm for 15 min at 4 ℃, and resuspended in the 10mM imidazole Bind buffer for sonication. The supernatant after centrifugation (10000 x *g* for 20 min) was purified with the HisTrap Kit and buffer kit (Amersham). The concentration of the purified protein was determined using the Bio-Rad protein assay reagent.

2.2. SDS-PAGE and Western blotting

The samples from fractions of each purification step were then dissolved in 2X SDS-PAGE sample buffer without 2-mercaptoethanol, and boiled for 10 min. Proteins were resolved on 12% SDS-PAGE gels and stained with Coomassie Brilliant Blue (Sigma).   Moreover, the electrophoretically separated proteins were transferred to nitrocellulose paper.   The resultant blots were blocked with 5% skim milk, and then reacted with the appropriately diluted Anti-His Tag monoclonal antibody (mAb) (Serotec) for a 3-h incubation. The blots were then washed with 1％ TBST three times and overlaid with a 1/5000 dilution of goat anti-mouse IgG antibodies conjugated with alkaline phosphatase (PerkinElmer Life Sciences,Inc.). Following a 1-h incubation at room temperature, the blots were developed with TNBT/BCIP (Gibco).

2.3. Azocasein digestion of SARS-CoV 3CL^{pro}

The protease activity of the SARS-CoV 3CL^{pro} was determined spectrophotometrically following the digestion of azocasein (Sigma) as the substrate [15].   150 μl of samples were added to 150 μl of chromogen reagent containing 2% azocasein in 50 mM Tris-HCl, pH 8.5.   After 2-h incubated at 37°C, non-digested azocasein was precipitated by adding 350 μl of 10% trichloroacetic acid (TCA) (Merck).   For determining the proteolytic activity, 350 μl of the resulting supernatants centrifuged at 10000 $\times g$ for 10 min was mixed with 300 μl 1 N NaOH, then was measured the absorbance of the above mixture at 440 nm.   The blank was obtained by precipitating the substrate plus the sample in TCA without incubation.

2.4. Site-directed mutagenesis of SARS-CoV 3CL^{pro}

His41, Cys145 and Glu166 within the catalytic sites of the SARS-CoV 3CL^{pro} protein were mutated by the PCR method as our previous report [16].   Site-directed mutagenesis was conducted by using paired complementary oligonucleotides for the desired point mutations to generate specific mutations into the SARS-CoV 3CL^{pro} protein.   The pairs of primers used were 5'-TGTCCAAGAGCCGTCATTTGC-3' and 5'-GCAAATGACGGCTCTTGGACA-3' for the substitution of His41 with alanine, 5'-AATGGATCAGCCGGTAGTGTT-3' and 5'-AACACTACCGGCTGATCCATT-3' for the replacement of Cys145 by alanine, and 5'-CATCATATGCGGCTTCCAACA-3' and 5'-TGTTGGAAGCCGCATATGATG-3' for the mutation of Glu166 with arginine. The correct sequence of each mutant of the SARS-CoV 3CL^{pro} protein constructs was confirmed using a DNA sequence analysis.

2.5. Construction and expression of SARS-CoV nsp7 fusion protein

The nsp7 gene located in the nucleotides 12937 to 13356 of the TW1 strain genome.   The cleavage substrate-I (S-I, TVRLQAGNATE) for the 3CL^{pro} protein located within the junction of nsp6 and nsp7, being fused at the N-terminus of the nsp7 protein (Fig. 1A).   The S-I/nsp7 gene was amplified using PCR with specific paired primers 5'-CGTGGATCCGGCTACAGTACGTCTTCAGGCT-3' and 5'-CGCAAGCTTGCGGAGTTGGTCACAACTACA-3'.   The forward primer mentioned above contained a *Bam*HI restriction site, and the reverse primers included a *Hind*III restriction site.   Each RT-PCR product was digested with *Bam*HI and *Hind*III, and then ligated into the *Bam*HI/*Hind*III cleavage sites of the pET43.1b vector (Novagen).   The resultant plasmids were transformed into the *E. coli* strain

BL21(DE3).   The S-I/nsp7 fusion protein expressed in *E. coli* was purified using the HisTrap Kit (Amersham).

2.6. In vitro trans-cleavage activity of the 3CL^pro determined by ELISA

For determining the *trans*-acting proteolytic assay, the SARS-CoV 3CL^{pro} reacted with the S-I/nsp7 fusion protein captured onto the microtiter plates (Fig. 1A).   The wells of a 96-well plate were coated with 100 µl of diluted anti-HSV mAb (Novagen) and incubated overnight at 4 ℃.   Following each incubation and subsequent layer of the ELISA, the wells were washed three times with TBS containing 0.05% Tween 20 (TBST).   After blocking by incubation with 5% skim milk in TBST for 2 h at room temperature (200 µl per well), 100 µl of the mixture containing the S-I/nsp7 fusion protein (10 µg/ml) and the 3CL^{pro} (300 µg/ml) was added into onto anti-HSV mAb-coated wells for the 3-hour incubation.   The intact form of the S-I/nsp7 fusion protein was detected using the S protein conjugated to peroxidase (Novagen) for 1 h at room temperature.   The ELISA products were developed with a chromogen solution containing 2,2'-azino-di-(3-ethylbenzthiazoline-6-sulfonate (ABTS) and hydrogen peroxide.   The relative *trans*-cleavage activity was calculated as $1 - (A405_{3CL}{}^{pro})/(A405_{no\ 3CL}{}^{pro})$.

2.7. The cell-based cis-cleavage activity of the 3CL^pro

For examining the *cis*-acting proteolytic assay, the 3CL^{pro} was fused in-frame with a cleavage site and a luciferase at the C-terminus (Fig. 1B).   The 3CL^{pro} gene was amplified using PCR with the paired primers 5'-CCCGGATCCAGTGGTTTTAGGAAAATGGCATTC-3' and 5'-TGCAGAATTCTTTCCTAAAACCACTCTGCAGAACAGCAGATTGGAAGGT AACACCAGAGCATTG-3'.   The forward primer mentioned above contained a *Bam*HI restriction site, and the reverse primer included an *Eco*RI restriction site and an in-frame gene encoding for the C-terminus of the 3CL^{pro} and the substrate II (S-II, SAVLQSGFRK).   The PCR product was digested with *Bam*HI and *Eco*RI, and then cloned into the pcDNA3.1 vector (Amersham).   The resulting plasmid was named as Pro/S-II.   Meanwhile, the substitutions of Leu and Gln in the substrate II by alanine with the plasmid Pro/S-II were also constructed using the reverse primers 5'-TGCAGAATTCTTTCCTAAAACCACTCTGCGCAACAGCAGA-3' and 5'-TGCAGAATTCTTTCCTAAAACCACTCGCCAGAACAGCAGA-3', which plasmids were designed as Pro/S-II(L->A) and Pro/S-II(Q->A), respectively.   Subsequently, the firefly luciferase gene in the pGL3(R2.1)-Basic vector (Promega) was amplified by PCR with the primers 5'-GGTGGAATTCATGGAAGACGCCAAAAACATAAAG-3' and 5'-TAGACTCGAGTTACACGGCGATCTTTCCGCCCTT-3'.   The luciferase gene

was cloned into the EcoR1/XhoI restriction enzyme sites of the plasmids Pro/S-II, Pro/S-II(L->A) and Pro/S-II(Q->A). These recombinant plasmids were designed as Pro/S-II/Luc, Pro/S-II(L->A)/Luc and Pro/S-II(Q->A)/Luc for detecting the *cis*-acting proteolytic activity of the 3CL^{pro} in Vero cells. Vero cells at 60-90% confluency in 6-well plates were transfected with 5 μg of total plasmids (0.5 μg of the indicated expression vector pEGFP-N1 plus 4.5 μg of pcDNA3.1, Pro/S-II, Pro/S-II/Luc, Pro/S-II(L->A)/Luc or Pro/S-II(Q->A)/Luc using the GenePorter reagent. According to manufacturer's direction (Gene Therapy Systems, San Diego,CA), the transfected cells were maintained in 2 ml of Dulbecco modified Eagle medium (DMEM) containing 20% bovine serum (FBS) after 5-hour incubation with the mixture of the plasmid DNA and GenePorter reagent. Transfected cells were selected using the DMEM containing 10 % FBS and 800 µg/ml of G418 for one month, and then G418-resistant cell clones were confirmed by the expression of green fluorescent protein (EGFP). Firefly luciferase activity in the transfected cells was measured using the dual Luciferase Reporter Assay System (Promega) and the Luminometer TROPIX TR-717 (Applied Biosystems).

3. Results

3.1. Expression and purification of the recombinant SARS-CoV 3CL^{pro} in E. coli

To examine the expression of the 3CL^{pro} protein in *E. coli*, the C-terminal His tagged 3CL^{pro} protein was detected using Western blotting with anti-His Tag monoclonal antibody. Western blot revealed that a 34 kD protein in the supernatant and the pellet fractions was found in the recombinant *E. coli* (data not shown). The 34-kDa recombinant protein was in agreement with the theoretical molecular weight (33.8 kDa) of the recombinant 3CL^{pro} fusion protein using the Compute pI/Mw tool (http://tw.expasy.org).

Subsequently, the soluble 3CL^{pro} protein expressed in the *E. coli* was harvested from the supernatant of the sonicated cells, and then purified using the immobilized-metal affinity chromatography (IMAC). The Coomassie Blue-stained gel revealed that one major band of the recombinant 3CL^{pro} protein was eluted with imidazole raging from 100 to 500 mM (Fig. 2A, lanes 5 to 9). The high purity of the 3CL^{pro} was observed in the last eluted fraction with 500 mM imidazole (Fig. 2A, lane 9). Interestingly, Western blotting demonstrated that an about 68-kDa immuno-reactive band, except a 34-kDa band, was found at more than 200 μg/ml concentration of our purified 3CL^{pro}, which was in the eluted fraction with imidazole ranging from 300, 400 and 500 mM (Fig. 2B, lanes 5 to 7). However, no immuno-reactive band was observed at lower than 200 μg/ml concentration, being in the eluted fraction with 200 mM imidazole (Fig. 2B, lane 4). The result was in

agreement with a previous report in that the purified SARS-CoV 3CL^{pro} at the more 200 μ g/ml protein concentration existed as a mixture of the inactive monomer (major) and the active dimer (minor) [13].

3.2. Azocasein hydrolysis of the SARS-CoV 3CL^{pro}

To test the protease activity of the recombinant 3CL^{pro} protein, the azocasein hydrolysis of the 3CL^{pro} protein in each eluted fraction was further performed (Fig. 2C). The azocasein proteolytic profile revealed that the 3CL^{pro} protein with a high purity eluted at 500 mM imidazole has highest proteolytic activity compared to those eluted fractions at 20, 40, 60, 100, and 300 mM imidazole (Fig. 2C). Moreover, the azocasein proteolytic assay showed a dose-dependent manner ability of the 3CL^{pro} protein using the serial 2-fold dilution ranging from 200 µg/ml to 800 µg/ml (data not shown). The results showed the enzyme activity of the purified 3CL^{pro} protein.

3.3. In vitro trans-cleavage activity of the 3CL^{pro}

The proteolytic specificity of the SARS-CoV 3CL^{pro} was examined using the in-vitro *trans*-cleavage of the substrate-I (S-I, TVRLQAGNATE mapped at the junction of nsp6 and nsp7). The substrate I was in-frame fused with a Nus-Tag and an S-Tag at the N-terminus and the nsp7 and an HSV-Tag at the C-terminus (Fig. 1A). According to the structure knowledge [17], mutations of His-41 by Ala (H41A), Cys-145 by Ala (C145A), and Glu-166 by Arg (E166R) within the substrate-binding site S1 were also performed and tested the effects on the enzyme activity. The t*rans*-cleavage of the S-I/nsp7 fusion protein (Nus Tag/S-Tag/S-I/nsp7/HSV-Tag) by the 3CL^{pro} and the mutants was analyzed using the Western blotting with the S-protein conjugated to peroxidase. An immuno-band for the cleavage product, the Nus Tag/S-Tag protein, was detected in the *trans*-cleavage by 3CL^{pro}, but not in the reactions by the 3CL^{pro} mutants H41A, C145A, E166R (data not shown). For quantification of the in vitro *trans*-cleavage, the mixture of the 3CL^{pro} and the S-I/nsp7 fusion protein was incubated in the anti-HSV mAb-coated wells. Subsequently, the non-cleavage form of the S-I/nsp7 fusion protein was captured and then detected using the ELISA with the S-protein conjugated to peroxidase (Fig. 3). The relative *trans*-cleavage ability revealed that the 3CL^{pro} mutants H41A, C145A, and E166R lose more than 50% activity compared to the wild type 3CL^{pro}. Furthermore, the enzyme activity of the 3CL^{pro} was significantly inhibited by the serine protease inhibitor 4-(2-aminoethyl)benzenesulfonyl fluoride hydrochloride (ABF) (Fig. 3). These results demonstrated the *trans*-cleavage specificity of the 3CL^{pro} and the importantly functional role of the residues His41, Cys145, and Glu166 within the substrate-binding site S1.

3.4. cis-cleavage activity of the 3CL^{pro} in the cell-based assays

For the cell-based *cis*-cleavage assay, the in-frame construction (Pro/S-II/Luc) of the 3CL^{pro}, the substrate-II (S-II, SAVLQSGFRK), and the luciferase plus pEGFP-N1 was transfected into Vero cells (Fig. 4D).   Since the fusion of the firefly luciferase with a more than 30 kDa protein fused as the N-terminus resulted in a dramatic decrease of luciferase activity [18], the detection of luciferase activity could be referred to the measurement of the *cis-* cleavage by the SARS-CoV 3CL^{pro}.   For examining the substrate specificity, alanine substitution of the substrate conserved residues Leu-$_{P2}$ and Gln-$_{P1}$, designed as Pro/S-II(L->A)/Luc and Pro/S-II(Q->A)/Luc, were also carried out (Fig. 4E and 4F).   Western blotting of the cell lysates with the anti-His Tag mAb demonstrated that three immuno-bands, a 94-kDa band for the fusion protein 3CL^{pro}/S-II/Luciferase, a 68-kDa band for the 3CL^{pro} dimer and a 34-kDa band for the 3CL^{pro} monomer, were clearly observed in the Vero cells transfected with Pro/S-II/Luc, Pro/S-II(L->A)/Luc, and Pro/S-II(Q->A)/Luc (data not shown).   However, the relative luciferase activity in the transfected cells showed that the Vero cells transfected with the plasmid Pro/S-II/Luc (100689 ± 408 light units) showed 4- and 25-fold higher luciferase activity compared to the cells carrying Pro/S-II(L->A)/Luc (23972 ± 582 light units) and Pro/S-II(Q->A)/Luc (3780 ± 282 light units), respectively (Fig. 4G).   The results demonstrated the *cis*-cleavage of the fusion protein 3CL^{pro}/substrate-II/luciferase.   Moreover, mutational analysis indicated that the conserved residue Gln at the P1 position mainly determined the substrate cleavage efficiency of the 3CL^{pro}.

4. Discussion

In this study, we demonstrated the expression and functional activity of the SARS-CoV 3CL^{pro} in *E. coli* and Vero cells, and also characterized the trans- and cis-cleavage of the substrates TVRLQAGNAT and SAVLQSGFRK in the fusion proteins by the 3CL^{pro}.   In addition, we examined the active site S1 and substrate specificity of the 3CL^{pro} using site-directed mutagenesis, providing the insight into molecular recognition of the SARS-CoV 3CL^{pro} with the substrates for the rational design of anti-SARS drugs.

Our results indicated that the recombinant SARS-CoV 3CL^{pro} exists a mixture of monomers (major) and dimers (minor) in the solutions (Fig. 2B), being in agreement with other studies on the recombinant protease of human coronavirus (HCoV) and the related porcine transmissible gastroenteritis (corona)virus (TGEV) [19, 20].   Furthermore, alanine substitution at the Cys145-His41 catalytic dyad resulted in the significant lose of the 3CL^{pro} enzyme activity (Fig. 3), revealing the

importance of the Cys145-His41 catalytic dyad. According to the crystallographic data [17], the Glu-166 in the substrate-binding subsite, S1, of the SARS-CoV 3CL^{pro} has a salt bridge with His172 and hydrogen bonds with the NH group of the other monomer Ser1, being important for the substrate binding and the 3CL^{pro} dimerization. Mutational analysis of Glu166 conformed the importance of Glu166 in the enzymatic function of the SARS-CoV 3CL^{pro} (Fig. 3). These results showed the important role of the substrate-binding subsite S1 in the anti-SARS drug design.

The identified cleavage site of the SARS-CoV 3CL^{pro} contains a LQA(S, N) motif recognized by most other coronavirus proteases [12, 21], which leads us to suggest the proteolytic processing of the SARS-CoV replicase polyproteins could be similar to those of other coronaviruses, such as HCoV and TGEV. Based on the conserved LQA(S, N) motif, Leu-$_{P2}$ and Gln-$_{P1}$ were selected for mutational analysis of the substrate specificity by the 3CL^{pro}. Alanine substitution at Leu-$_{P2}$ and Gln-$_{P1}$ revealed that Gln-$_{P1}$ dominantly determined the cleavage efficiency of the substrates by the SARS-CoV 3CL^{pro} (Fig. 4G). We will further characterize the substrate specificity by the systematically mutational analysis for the molecular-based design on the anti-SARS drugs.

In this study, we establish the in vitro *trans*-cleavage assay and the cell-based *cis*-cleavage assay with the recombinant 3CL^{pro} protein. The azocasein and the substrate fusion protein Nus-Tag/S-Tag/S-I/nsp7/HSV-Tag were used as the substrates in the in vitro *trans*-cleavage assay, providing the rapid and quantifiable assay for large-scale screening of SARS-CoV 3CL^{pro} inhibitors. Furthermore, the luciferase activity referred to the cell-based *cis*-cleavage activity will be useful for the examination of the inhibitory effects on the SARS-CoV 3CL^{pro} in the Vero cells. Therefore, this study not only characterizes the molecular interaction of the SARS-CoV 3CL^{pro} with the substrates, but also provides reliable assays for screening the anti-SARS drugs.

References

1. Poutanen, S. M., Low, D. E., Henry, B., Finkelstein, S., Rose, D., Green, K., Tellier, R., Draker, R., Adachi, D., Ayers, M., Chan, A. K., Skowronski, D. M., Salit, I., Simor, A. E., Slutsky, A. S., Doyle, P. W., Krajden, M., Petric, M., Brunham, R. C., and McGeer, A. J. (2003) N. Engl. J. Med. 348, 1995-2005.
2. Lee, N., Hui, D., Wu, A., Chan, P., Cameron, P., Joynt, G. M., Ahuja, A., Yung, M. Y., Leung, C. B., To, K. F., Lui, S. F., Szeto, C. C., Chung, S., and Sung, J. J. (2003) N. Engl. J. Med. 348, 1986-1994.
3. Tsang, K. W., Ho, P. L., Ooi, G. C., Yee, W. K., Wang, T., Chan-Yeung, M., Lam, W. K., Seto, W. H., Yam, L. Y., Cheung, T. M., Wong, P. C., Lam, B., Ip, M. S., Chan, J., Yuen, K. Y., and Lai, K. N. (2003) N. Engl. J. Med. 348, 1977-1985.
4. Hsueh, P. R., Chen, P. J., Hsiao, C. H., Yeh, S. H., Cheng, W. C., Wang, J. L., Chiang, B. L., Chang, S. C., Chang, F. Y., Wong, W. W., Kao, C. L., and Yang, P. C. (2004) Emerg. Infect. Dis. 10, 489-493.
5. Ksiazek, T. G., Erdman, D., Goldsmith, C. S., Zaki, S. R., Peret, T., Emery, S., Tong, S., Urbani, C., Comer, J. A., Lim, W., Rollin, P. E., Dowell, S. F., Ling, A. E., Humphrey, C. D., Shieh, W. J., Guarner, J., Paddock, C. D., Rota, P., Fields, B., DeRisi, J., Yang, J. Y., Cox, N., Hughes, J. M., LeDuc, J. W., Bellini, W. J., and Anderson, L. J. (2003) N. Engl. J. Med. 348, 1953-1966.
6. Peiris, J. S., Chu, C. M., Cheng, V. C., Chan, K. S., Hung, I. F., Poon, L. L., Law, K. I., Tang, B. S., Hon, T. Y., Chan, C. S., Chan, K. H., Ng, J. S., Zheng, B. J., Ng, W. L., Lai, R. W., Guan, Y., and Yuen, K. Y. (2003) Lancet 361, 1767-1772.
7. Drosten, C., Gunther, S., Preiser, W., van der Werf, S., Brodt, H. R., Becker, S., Rabenau, H., Panning, M., Kolesnikova, L., Fouchier, R. A., Berger, A., Burguiere, A. M., Cinatl, J., Eickmann, M., Escriou, N., Grywna, K., Kramme, S., Manuguerra, J. C., Muller, S., Rickerts, V., Sturmer, M., Vieth, S., Klenk, H. D., Osterhaus, A. D., Schmitz, H., Doerr, H. W. (2003) N. Engl. J. Med. 348, 1967-1976.
8. Lai, M. M. C., and Holmes, K. V. (2001) in: Fields Virology (Knipe, D. M. and Howley, P.M., Eds) Lippincott Williams and Wilkins, New York.
9. Enjuanes, L., Brian, D., Cavanagh, D., Holmes, K., Lai, M. M. C., Laude, H., Masters, P., Rottier, P., Siddell, S. G. Spaan, W. G. M., Taguchi, F., and Talbot, P. (2000) in: Virus Taxonomy (van Regenmortal, M. H. V., Fauqet, C. M., Bishop, D. H. L., Carstens, E. B., Estes, M. K., Lemon, S. M., Mayo, M. A., McGeoch, D. J., Pringle, C. R., and Wickner, R. B., Eds) Academin Press, New York.
10. Holmes, K. V. (2001) in: Fields Virology (Knipe, D. M. and Howley, P.M., Eds) Lippincott Williams and Wilkins, New York.
11. Ziebuhr, J., Snijder, E. J., and Gorbalenya, A. E. (2000) J. Gen. Virol. 81, 853-879.
12. Gao, F., Ou, H. Y., Chen, L. L., Zheng, W.X., and Zhang, C. T. (2003) FEBS Lett. 553, 451-456.
13. Fan, K., Wei, P., Feng, Q., Chen, S., Huang, C., Ma, L., Lai, B., Pei, J., Liu, Y., Chen, J., and Lai, L. (2004) J. Bio. Chem. 279, 1637-1642
14. Hsueh, P. R., Hsiao, C. H., Yeh, S. H., Wang, W. K., Chen, P. J., Wang, J. T., Chang, S. C., Kao, C. L., Yang, P. C. (2003) Emerg. Infect. Dis. 9, 1163-1167.
15. Tomarelli, R. M., Charney, J., and Harding, M. L. (1949) J. Lab. Clin. Med. 34, 428–433.

16. Lin, C. W., and Wu, S. C. (2003) J. Virol. 77, 2600-2606.
17. Yang, H., Yang, M., Ding, Y., Liu, Y., Lou, Z., Zhou, Z., Sun, L., Mo, L., Ye, S., Pang, H., Gao, G. F., Anand, K., Bartlam, M., Hilgenfeld, R., and Rao, Z. (2003) Proc. Natl. Acad. Sci. USA 100, 13190-13195.
18. Joubert, P., Pautigny, C., Madelaine, M. F., and Rasschaert, D. (2000) J. Gen. Virol. 81, 481-488.
19. Anand, K., Palm, G. J., Mesters, J. R., Siddell, S. G., Ziebuhr, J., and Hilgenfeld, R. (2002) EMBO J. 21, 3213-3224.
20. Anand, K., Ziebuhr, J., Wadhwani, P., Mesters, J. R., and Hilgenfeld, R. (2003) Science 300, 1763-1767.
21. Hegyi, A., and Ziebuhr, J. (2002) J. Gen. Virol. 83, 595-599.

Figure Caption

Fig. 1.　Flowcharts for the in vitro *trans*-cleavage ELISA assay (A) and the cell-based *cis*-cleavage luciferase assay (B).　For *trans*-cleavage assay (A), the substrate-I/nsp7 (S-I/nsp7) gene was cloned into the pET43.1b expression vector for generation of the in-frame S Tag-nsp7-HSV Tag fusion proteins in *E. coli*. Subsequently, the *trans*-cleavage product of the fusion protein S-I/nsp7 by the 3CL^{pro} and the mutants (H41A, C145A, and E166R) was captured onto the anti-HSV mAb coated microwells.　The non-cleavage fusion protein was detected using the S protein-HRP conjugate and ABTS/H_2O_2 substrates.　For *cis*-cleavage assay (B), the in-frame construction of the 3CL^{pro}, the substrate-II, and luciferase plus the pEGFP-N1 was transfected into the Vero cells.　The luciferase activity was referred to monitor the *cis*-cleavage of the fusion protein the 3CL^{pro}-substrate-II-luciferase.

Fig. 2.　SDS-PAGE (A), Western blotting (B), and enzyme activity (C) of the recombinant SARS-CoV 3CL^{pro} in each purified step.　(A) The supernatant of the sonicated cells transformed with the pET24a-3CL^{pro} plasmid was purified by IMAC. 20 μl of each eluted fraction was analyzed by 12% SDS-PAGE with Coomassie blue staining.　Lanes 2 to 9 indicated the samples from the fractions eluted with 20, 40, 60, 100, 200, 300, 400, and 500 mM imidazole, respectively.　Lane 1 was the molecular marker.　kD, kilodaltons.　(B) 5 μl of each eluted fraction was analyzed by 12% SDS-PAGE, then electrophorectically transferred onto nitrocellulose paper.　The blot was probed with mouse anti-His tag antibodies, and developed with an alkaline phosphatase- conjugated secondary antibody and NBT/BCIP substrates.　Lanes 2 to 7 indicated the samples from the fractions eluted with 60, 100, 200, 300, 400, and 500 mM imidazole, respectively.　(C) The digestion of azocasein by the 3CL^{pro} protein was measured at 440 nm.　The blank was obtained by precipitating the substrate plus the sample in TCA without incubation.
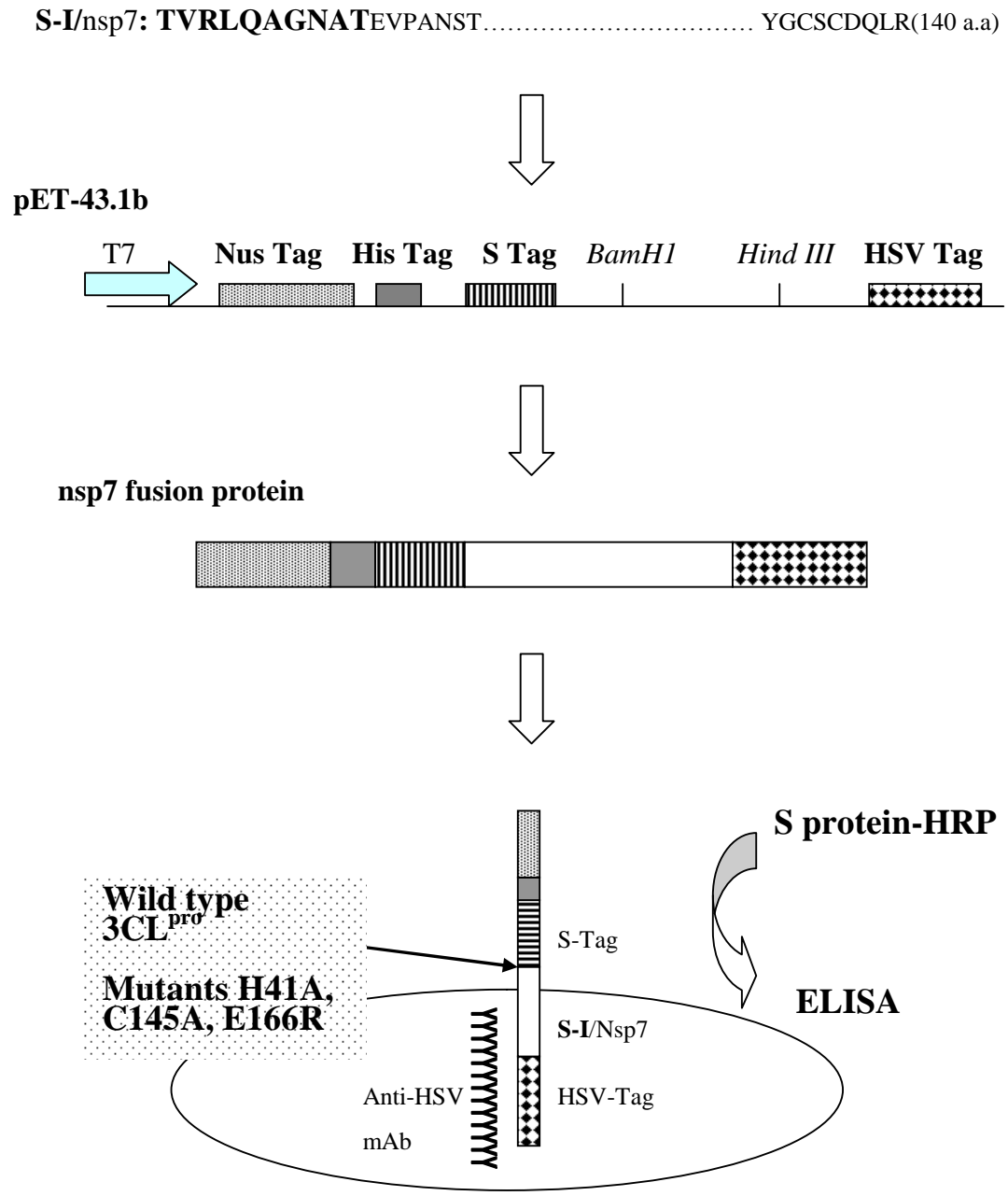
Fig. 3.　ELISA for the *trans*-cleavage of the S-I/nsp7 fusion protein by the 3CL^{pro} and the mutants H41A, C145A, and E166E.　After the 3-hour incubation, the mixture of the fusion protein Nus-Tag/S-Tag/S-I/nsp7/HSV-Tag and the 3CL^{pro} was added into the anti-HSV mAb-coated wells. The inhibitor 4-(2-aminoethyl)benzenesulfonyl fluoride hydrochloride (ABF) was also added into the *trans*-cleavage assay.　The non-cleavage S-I/nsp7 fusion protein captured onto 96-well plates with anti-HSV mAb was detected using the S protein-HRP conjugate and ABTS/H_2O_2 substrates. The ELISA product was measured at A405 nm.　The relative *trans*-cleavage activity was calculated as $1 - (A405_{3CL}^{pro})/(A405_{no\ 3CL}^{pro})$.

Fig. 4. Expression of the in-frame gene 3CL^{pro}/S-II/Luc for the *cis*-cleavage analysis. (A to F) Microscopical analysis of the Vero cells with bright field (left) and fluorescent light (right). Vero cells (B to F) transfected with pEGFP-N1 plus pcDNA3.1, Pro/S-II, Pro/S-II/Luc, Pro/S-II(L->A)/Luc or Pro/S-II(Q->A)/Luc were compared to the un-transfected cells (A). (G) Equal amounts (100 μg) of cell lysates were used to determine the luciferase activity using the dual Luciferase Reporter Assay System. The reference cells transfected with pcDNA3.1 or Pro/S-II were used to subtract background noise. Relative luciferase activity in the test cells transfected with Pro/S-II/Luc, Pro/S-II(L->A) or Pro/S-II(Q->A)/Luc was determined as the value of light units$_{test-reference}$.

Fig. 1.

(A)

S-I/nsp7: **TVRLQAGNAT**EVPANST……………………………… YGCSCDQLR(140 a.a)

pET-43.1b

T7   **Nus Tag**   **His Tag**   **S Tag**   *BamH1*   *Hind III*   **HSV Tag**

nsp7 fusion protein

S protein-HRP

Wild type 3CL^pro

Mutants H41A, C145A, E166R

S-Tag

S-I/Nsp7

Anti-HSV

mAb

HSV-Tag

ELISA

16

Fig. 1.

(B)
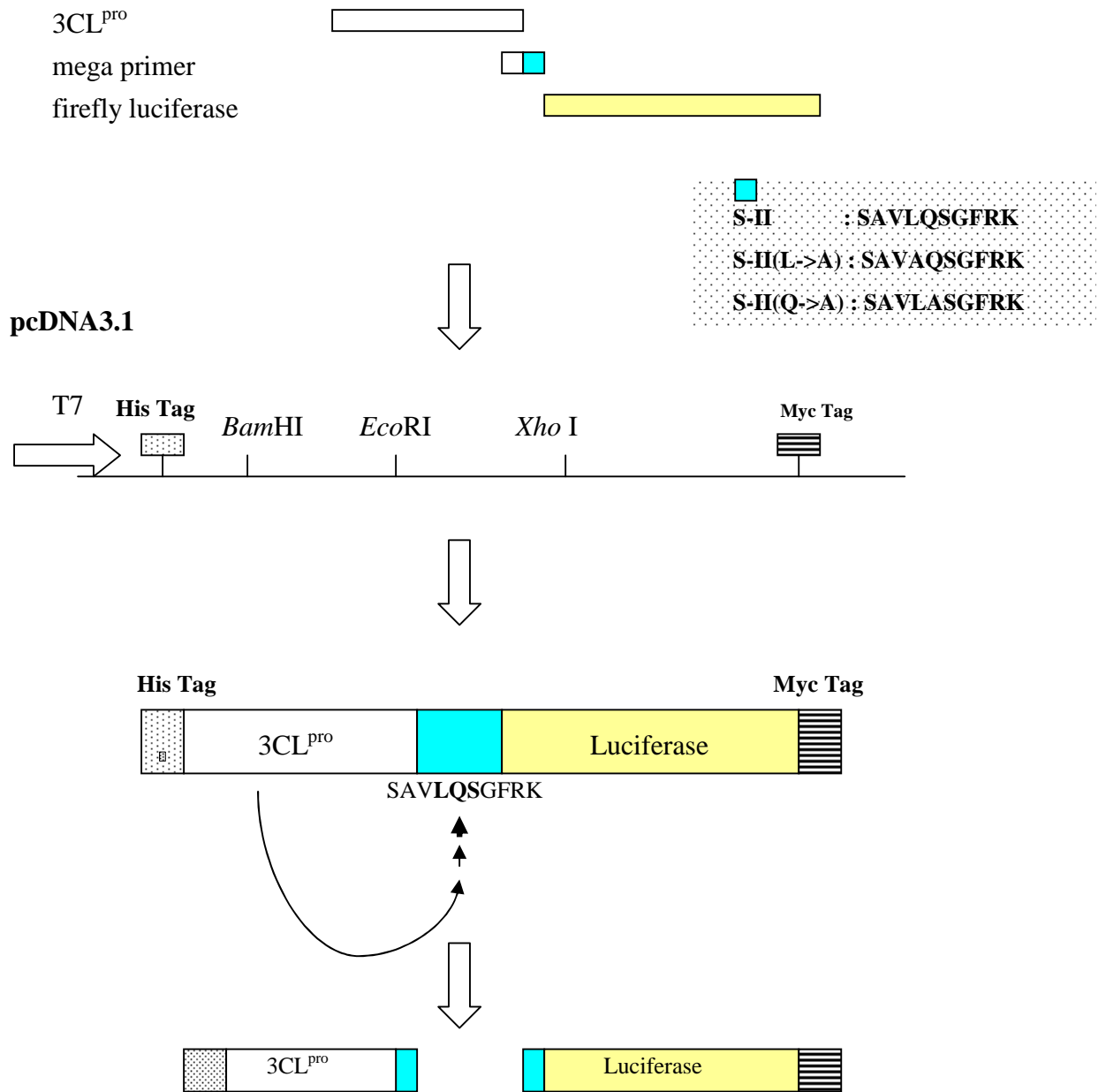
Firefly luciferase activity assay
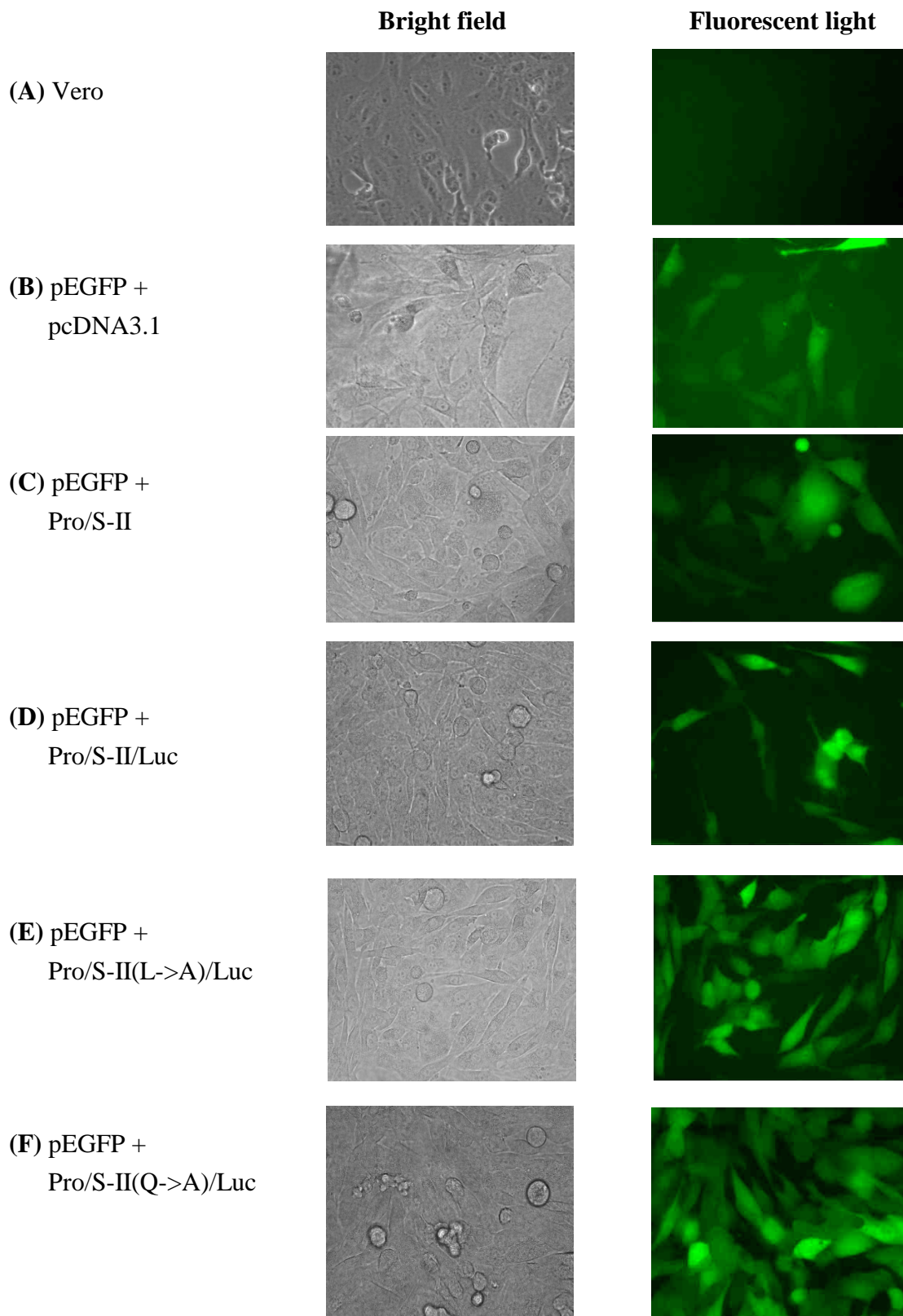
Fig. 2.

(A)

Fig. 2.

(B)

MW (kDa)	1	2	3	4	5	6	7	
100 →								
72 →								← **Dimer**
55 →								
40 →								
33 →								← **Monomer**
24 →								
17 →								

Eluted by   *60*   *100*   *200*   *300*   *400*   *500*   *mM Imidazole*

Fig. 2.

(C)

Fig. 3.

Fig. 4.

	Bright field	Fluorescent light
(A) Vero		
(B) pEGFP + pcDNA3.1		
(C) pEGFP + Pro/S-II		
(D) pEGFP + Pro/S-II/Luc		
(E) pEGFP + Pro/S-II(L->A)/Luc		
(F) pEGFP + Pro/S-II(Q->A)/Luc		
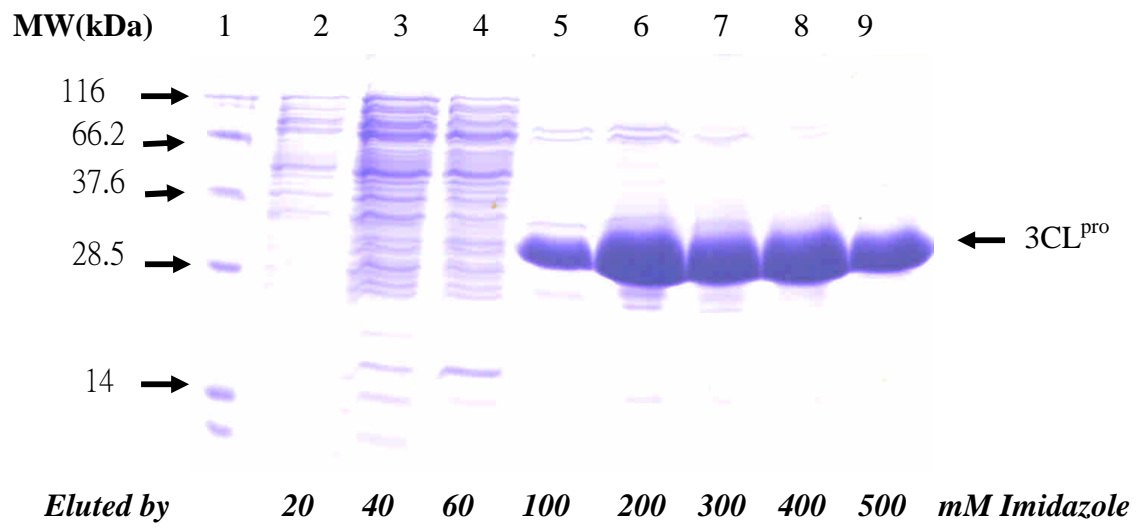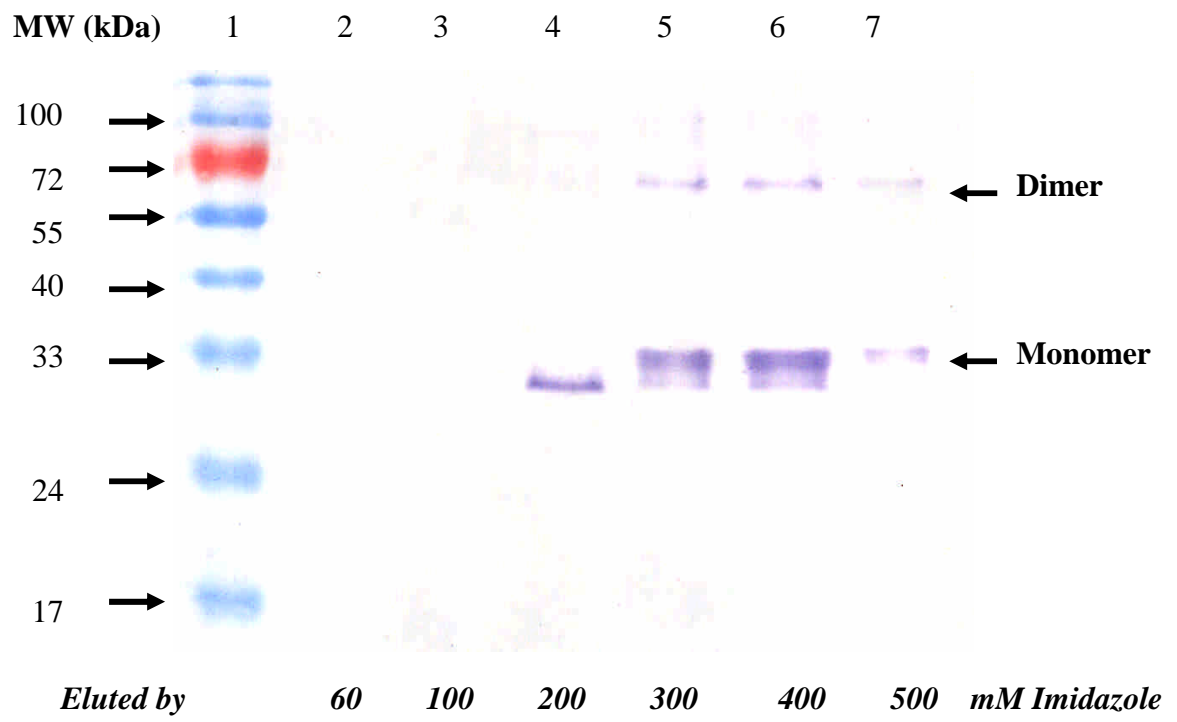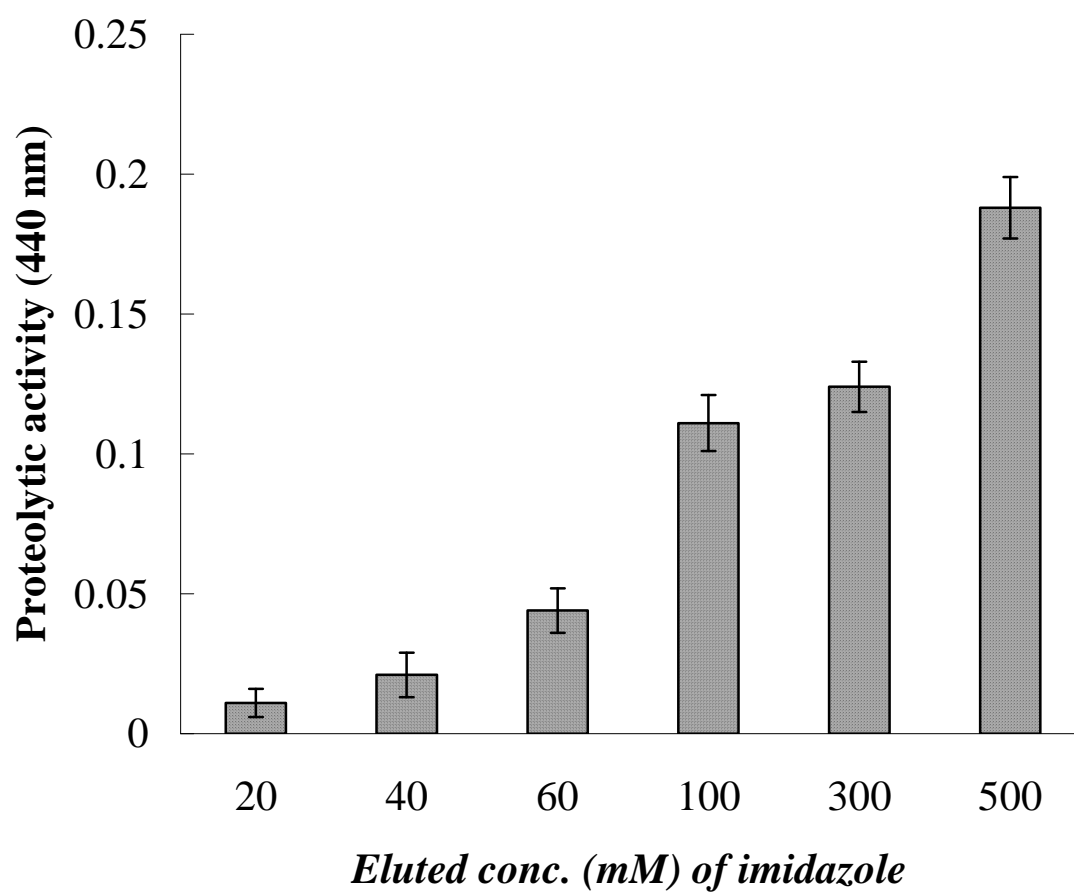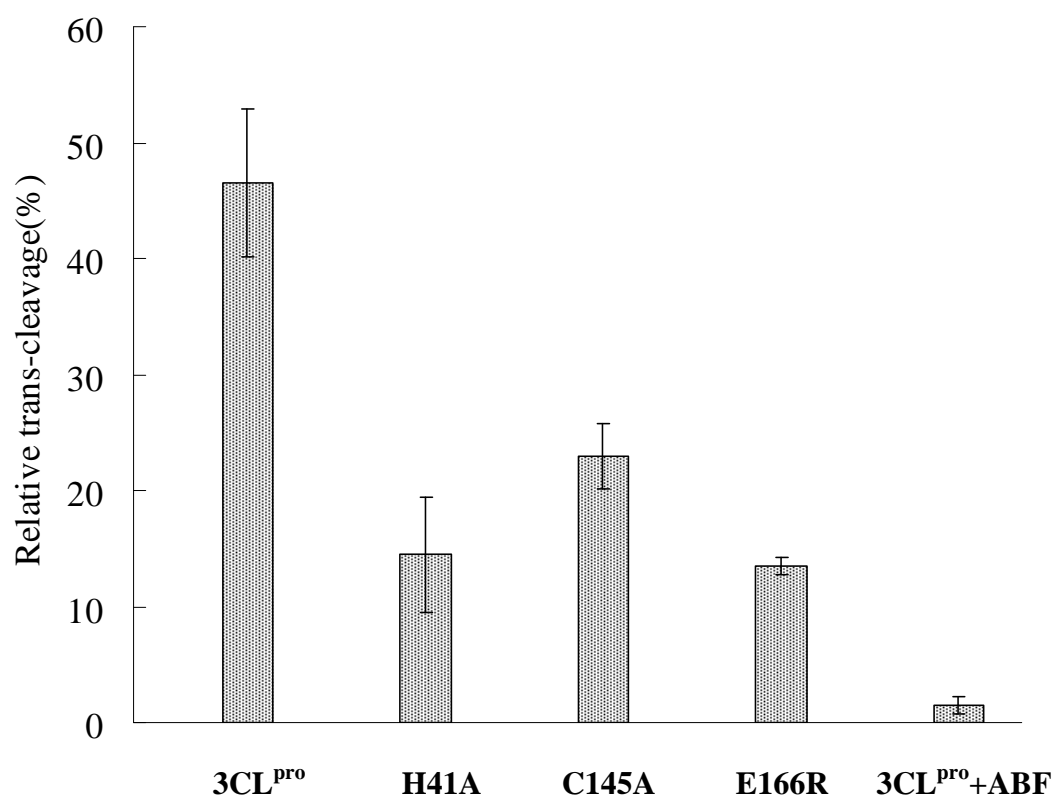
Fig. 4.

(G)

Part II: **Studies on the Anti- SARS Coronavirus 3C-like Protease Effect of the** *Isatis Indigotica* **Root**

1. Introduction

Severe acute respiratory syndrome (SARS) was rapidly transmitted through aerosols, causing 8,447 reported cases with 811 deaths worldwide in a short period from February to June, 2003 [1-3]. A novel coronavirus, SARS-coronavirus (SARS-CoV) was identified as the etiological agent of the disease [4-7]. SARS-CoV particles contain a single positive-stranded RNA genome that is approximately 30 kb in length and has a 5' cap structure and 3' polyA tract [8-10]. The SARS-CoV genome encodes for replicase, spike, envelope, membrane, and nucleocapsid. The replicase gene encodes two large overlapping polypeptides (replicase 1a and 1ab, ~ 450kD and ~750kD, respectively), including 3C-like protease (3CL[pro]), RNA-dependent RNA polymerase, and RNA helicase for viral replication and transcription [11]. The SARS-CoV 3CL[pro] mediates the proteolytic processing of replicase polypeptides 1a and 1ab into functional proteins, playing an important role in viral replication. Therefore, the SARS-CoV 3CL[pro] becomes an attractive target for developing effective drugs against SARS.

Isatis Indigotica Root (*Radix Isatidis*), belonging to the family Crucuferae, is native to China. The root of *Isatis Indigotica*, popularly known as Ban-Lan-Gen in Chinese, is used in tranditional Chinese medicine for febrile diseases, mumps, erysipelas, and inflammatory diseases [12]. The antiviral effects of *Isatis Indigotica* Root were found against influenza, hepatitis and Japanese encephalitis [13, 14]. During epidemic SARS in Hong Kong and China, the dried root of *Isatis Indigotica* was one of the popular Chinese herbs for the prevention of the atypical pneumonia, even being used for the treatment of SARS. The *Isatis Indigotica* Root contains indigo, indirubin, indican (indoxyl-β-D-glucoside), β-sitosterol, γ-sitosterol, sinigrin, etc. Indirubin, a by-product of indigo synthesis, was identified as an anti-leukemia active ingredient [15, 16] and an inhibitor of cyclin-dependent kinases [17]. Interestingly, indigo and indirubin were also identified as the promiscuous non-kinase enzyme inhibitors for β-lactamase, chymotrypsin, and malate dehydrogenase [18]. The β-sitosterol showed the strong inhibitory effects on protein tyrpsone kinase [19] and 5alpha-reductase [20].

In this study, we characterized the anti-SARS CoV 3CL[pro] effect of the extract and the compounds of the *Isatis Indigotica* Root using the in vitro *trans*-cleavage ELISA and cell-based *cis*-cleavage luciferase assay. The results showed that the *Isatis Indigotica* Root extract significantly inhibited the enzymatic actvity of 3CL[pro] in the in vitro and in vivo assay. In addition, the potential compounds indigo, sinigrin

and beta-sitpsterol exhibited the anti-SARS CoV 3CL^{pro} in dose-dependent manners. The study not only demonstrates the anti-SARS CoV activity of *Isatis Indigotica* Root, but also provides high throughput methods for screening the anti-SARS inhibitors.

2. Materials and Methods

2.1. Construction, expression, and purification of SARS-CoV 3CL^{pro}

The 3CL^{pro} gene located within the nucleotides 9985 to 10902 of the SARS-CoV TW1 strain genome (GenBank accession No. AY291451) [21] was amplified using the reverse-transcriptase polymerase chain reaction (RT-PCR) with specific primers 5'-CCCGGATCCAGTGGTTTTAGGAAAATGGCATTC-3' and 5'-GGTGCTCGAGTTGGAAGGTAACACCAGAGCATTG-3'. The forward primer mentioned above contained an *Eco*RI restriction site, and the reverse primers included an *Xho*I restriction site. Each RT-PCR product was digested with *Eco*RI and *Xho*I, and then ligated into the *Eco*RI/*Xho*I cleavage sites of the pET24a vector (Novagen) and expressed as a histidine tag fusion protein. The *E. coli* strain BL21(DE3) was transformed with the resulting plasmid, pET24a-3CL^{pro}, then cultured in LB medium in the presence of 100 μg of kanamycin per ml at 37℃. Once the cultures reached an absorbance at 600nm of 0.5 to 0.6, they were induced by the addition of 4 mM isopropyl-β-D-thiogalactopyranoside (IPTG) for 4 h at 22℃. Finally, the bacteria were harvested by centrifugation at 10000 rpm for 15 min at 4℃, and resuspended in the 10mM imidazole Bind buffer for sonication. The supernatant after centrifugation (10000 x g for 20 min) was purified with the HisTrap Kit and buffer kit (Amersham). The concentration of the purified protein was determined using the Bio-Rad protein assay reagent.

2.2. SDS-PAGE and Western blotting

The samples from fractions of each purification step were then dissolved in 2X SDS-PAGE sample buffer without 2-mercaptoethanol, and boiled for 10 min. Proteins were resolved on 12% SDS-PAGE gels and stained with Coomassie Brilliant Blue (Sigma). Moreover, the electrophoretically separated proteins were transferred to nitrocellulose paper. The resultant blots were blocked with 5% skim milk, and then reacted with the appropriately diluted Anti-His Tag monoclonal antibody (mAb) (Serotec) for a 3-h incubation. The blots were then washed with 1％ TBST three times and overlaid with a 1/5000 dilution of goat anti-mouse IgG antibodies conjugated with alkaline phosphatase (PerkinElmer Life Sciences,Inc.). Following a 1-h incubation at room temperature, the blots were developed with TNBT/BCIP (Gibco).

2.3. In vitro trans-cleavage activity of the 3CL^{pro} determined by ELISA

The cleavage substrate I (S-I, TVRLQAGNATE) for the 3CL^{pro} protein was synthesized as the S-1/nsp7 fusion protein with the N-terminal S-Tag and C-terminal HSV Tag and His-Tag [22]. For determining the *trans*-acting proteolytic assay, the SARS-CoV 3CL^{pro} reacted with the S-I/nsp7 fusion protein captured onto the microtiter plates. The wells of a 96-well plate were coated with 100 µl of diluted anti-HSV mAb (Novagen) and incubated overnight at 4 ℃. Following each incubation and subsequent layer of the ELISA, the wells were washed three times with TBS containing 0.05% Tween 20 (TBST). After blocking by incubation with 5% skim milk in TBST for 2 h at room temperature (200 µl per well), 100 µl of the mixture containing the S-I/nsp7 fusion protein (10 µg/ml) and the 3CL^{pro} (10 µg/ml) was added into onto anti-HSV mAb-coated wells for the 3-hour incubation. The intact form of the S-I/nsp7 fusion protein was detected using the S protein conjugated to peroxidase (Novagen) for 1 h at room temperature. The ELISA products were developed using a chromogen solution containing 2,2'-azino-di-(3-ethylbenzthiazoline-6-sulfonate (ABTS) and hydrogen peroxide and then measured at A405 nm. The relative *trans*-cleavage activity was calculated as $1 - (A405_{3CL}{}^{pro})/(A405_{no\ 3CL}{}^{pro})$.

2.4. The cell-based cis-cleavage activity of the 3CL^{pro}

For examining the *cis*-acting proteolytic assay, the 3CL^{pro} was fused in-frame with a cleavage site and a luciferase at the C-terminus described in our previous report [22]. The resulting plasmid pcDNA3.1- Pro/S-II/Luc plus the indicated expression vector pEGFP-N1was transited into Vero cells using the GenePorter reagentording to manufacturer's direction (Gene Therapy Systems, San Diego,CA), the transfected cells were maintained in 2 ml of Dulbecco modified Eagle medium (DMEM) containing 20% bovine serum (FBS) after 5-hour incubation with the mixture of the plasmid DNA and GenePorter reagent. Transfected cells were selected using the DMEM containing 10 % FBS and 800 µg/ml of G418 for one month, and then G418-resistant cell clones were confirmed by the expression of green fluorescent protein (EGFP). If the cis-cleavage of the 3CL^{pro} occurs, firefly luciferase activity in the transfected cells will be measured using the dual Luciferase Reporter Assay System (Promega) and the Luminometer TROPIX TR-717 (Applied Biosystems).

2.5. Extracts and compounds of Isatis Indigotica Root

The root of *Isatis Indigotica* purchased from Sun Ten Pharmaceutical Corporation (Taiwan) was ground with homogenizer to a fine powder. The extract was prepared by mixing 3 g of each herb powder with 10 ml of water and boiling at 80 ℃ for 30

min.   After being centrifuged at 10,000×g for 5 min, and the supernatant of the extract was evaporated under vacuum to dryness and resuspended in water to a final concentration of 1 mg/ml.   Indigo and indirubin were kindly provided by Dr. Yuan-Shiun Chang, professor for Institute of Chinese Pharmaceutical Sciences, China Medical University.   Indican (indoxyl-β-D-glucoside), β-sitosterol, and sinigrin were purchased from Sigma Chemical.

2.7. Cell proliferation (MTT) assay

The suspended Vero cells in MEM medium with 10 % FBS were plated in 96-well plates (1*10^4 cells/well) and then treated with the indicated compounds. After the treatment at 37 ℃ in 5% CO_2 for 20 h,   25 μl of a MTT solution at 5 mg/ml was added to each well and incubated at 37 ℃ in 5% CO_2 for 3 h. Subsequently washing with three times of phosphate buffer saline, 100 μl DMSO was then added into the plates for dissolveing the formazan crystals. $OD_{570-630}$ in each well was then measured with a micro-ELISA reader.

3. Results and discussion

3.1. Monomer and dimer of the recombinant SARS-CoV 3CL^{pro}

To examine monomer and dimer of the synthesized 3CL^{pro} protein in *E. coli*, the purified 3CL^{pro} protein at the 1 mg/ml concentration was analyzed using SDS-PAGE and Western blotting (Fig. 1).   The Coomassie Blue-stained gel revealed that a major 34-kDa band for the monomer and a minor 68-kDa band for the dimer were observed (Fig. 1A, lane 2).   Western blotting with the anti-His tag monoclonal antibody clearly indicated the 68-kDa immuno-reactive band at the 1 mg/ml concentration of our purified 3CL^{pro} (Fig. 1B, lane 2).   The result demonstrated the mixture of monomer and dimer at the 1 mg/ml concentration of the purified SARS-CoV 3CL^{pro}.

For characterizing the in vitro *trans*-cleavage, the cleavage of the S-I/nsp7 fusion protein by the 3CL^{pro} was detected using the ELISA.   The in vitro trans-cleavage assay showed a dose-dependent manner ability of the 3CL^{pro} protein using the serial 2-fold dilution ranging from 200 μg/ml to 1000 μg/ml (data not shown).   For the *cis*-cleavage assay, the in-frame construction of the 3CL^{pro}, the substrate-II, and the luciferase, designed as the plasmid pcDNA3.1-3CL^{pro}-/S-II/Luc, was transfected into Vero cells.   Since the fusion of the firefly luciferase with a more than 30 kDa protein fused as the N-terminus resulted in a dramatic decrease of luciferase activity [23], the detection of luciferase activity could be referred to the measurement of the *cis*- cleavage by the SARS-CoV 3CL^{pro}.   Western blotting with the ant-luciferase monoclonal antibody showed a 94-kDa band for the fusion protein 3CL^{pro}-S-II-Luciferase and a 60-kDa band for the luciferase in the Vero cells

transfected with the plasmid pcDNA3.1-3CL^{pro}/S-II/Luc (Fig. 2, lanes 3 to 5). The result demonstrated the cis-cleavage activity of the 3CL^{pro} in Vero cells.

3.2. Inhibitory effects on the SARS-CoV 3CL^{pro} by Isatis Indigotica Root

To evaluate the anti-3CL^{pro} effect, the extract of *Isatis Indigotica* Root was tested using the in vitro *trans*-cleavage and cell-based *cis*-cleavage assays. For the *trans*-cleavage assay, the extract of *Isatis Indigotica* Root showed a dose-dependent anti-3CL^{pro} effect with the 50% inhibitory concentration (IC$_{50}$) of 80.3 ± 4.2 μg/ml (Fig. 3, Table 1). For the *cis*-cleavage assay, the extract of *Isatis Indigotica* Root significantly inhibited the cis-cleavage activity of the SARS-CoV 3CL^{pro} in Vero cells with the IC$_{50}$ value of 191.6 ± 8.2 μg/ml (Fig. 4, Table 2). The IC$_{50}$ of the *Isatis Indigotica* root extract for the *cis*-cleavage in Vero cells was 2-fold higher than the IC$_{50}$ value for the in vitro *trans*-cleavage, which reason may be due to the different action of the *Isatis Indigotica* root extract in the in vitro and in vivo assays. The results demonstrated the significant effect of the *Isatis Indigotica* root extract on the anti-SARS in vitro and in vivo.

3.3. Anti-3CL^{pro} effects of the compounds in the *Isatis Indigotica* root

To examine the potential compounds against SARS, five compounds of the *Isatis Indigotica* root, including indigo, indirubin, indican, sinigrin, and beta-sitosterol were further tested using the in vitro and in vivo cleavage assays of the SARS-CoV 3CL^{pro} (Figs 5 and 6, Tables 1 and 2). For the in vitro *trans*-cleavage assay, the five compounds had a significant effect on the inhibition of the 3CL^{pro} enzyme activity. The order of the IC50 value for the in vitro assay was indican (112 μM), beta-sitosterol (115 μM), sinigrin (121 μM), indirubin (293 μM), and indigo (300 μM) (Fig.5 and Table 1). Furthermore, beta-sitosterol, sinigrin, and indigo significantly inhibited the cell-based cis-cleavage of the 3CL^{pro} in a dose-dependent manner (Fig. 6). But, no dose-dependent inhibition on the cis-cleavage in Vero cells was found for indirubin and indican. The difference on the inhibitory effect of the trans- and cis-cleavage by indirubin and indican may be due to that these two compounds stimulated the proliferation of Vero cells, being determined using the MTT assay (Table 2). The result indicated the in vitro and in vivo anti-3CL^{pro} effect of indigo, sinigrin, and beta-sitosterol with the low toxicity.

In this study, we demonstrated the anti-SARS CoV 3CL^{pro} effect by the water extract of the *Isatis Indigotica* root with the IC$_{50}$ values of 80.3 μg/ml for the in vitro assay and 191.6 μg/ml for the in vivo assay (Figs 3 to 6, Tables 1 and 2). At the concentration of 500 μg/ml, the *Isatis Indigotica* root extract showed 93% of MTT metabolism compared to the untreated Vero cells (Table 2). In addition, the five

compounds of the *Isatis Indigotica* root indicated a significant effect on the in vitro inhibition of the 3CL^{pro} enzyme activity at least at micromolar concentrations.   The results indicated the therapeutic value of the *Isatis Indigotica* root against SARS. The combination of the *Isatis Indigotica* root with the reported potential anti-SARS compounds, such as glycyrrhizin [24], nelfinavir [25], aurintricarboxylic acid [26], and interferon [27] could be alternative approaches for the treatment of the SARS patients.

Reference

[1] Ksiazek, T. G., Erdman, D., Goldsmith, C. S., Zaki, S. R., Peret, T., Emery, S., Tong, S., Urbani, C., Comer, J. A., Lim, W., Rollin, P. E., Dowell, S. F., Ling, A. E., Humphrey, C. D., Shieh, W. J., Guarner, J., Paddock, C. D., Rota, P., Fields, B., DeRisi, J., Yang, J. Y., Cox, N., Hughes, J. M., LeDuc, J. W., Bellini, W. J., and Anderson, L. J. (2003) N. Engl. J. Med. 348, 1953-1966.

[2] Peiris, J. S., Chu, C. M., Cheng, V. C., Chan, K. S., Hung, I. F., Poon, L. L., Law, K. I., Tang, B. S., Hon, T. Y., Chan, C. S., Chan, K. H., Ng, J. S., Zheng, B. J., Ng, W. L., Lai, R. W., Guan, Y., and Yuen, K. Y. (2003) Lancet 361, 1767-1772.

[3] Drosten, C., Gunther, S., Preiser, W., van der Werf, S., Brodt, H. R., Becker, S., Rabenau, H., Panning, M., Kolesnikova, L., Fouchier, R. A., Berger, A., Burguiere, A. M., Cinatl, J., Eickmann, M., Escriou, N., Grywna, K., Kramme, S., Manuguerra, J. C., Muller, S., Rickerts, V., Sturmer, M., Vieth, S., Klenk, H. D., Osterhaus, A. D., Schmitz, H., Doerr, H. W. (2003) N. Engl. J. Med. 348, 1967-1976.

[4] Poutanen, S. M., Low, D. E., Henry, B., Finkelstein, S., Rose, D., Green, K., Tellier, R., Draker, R., Adachi, D., Ayers, M., Chan, A. K., Skowronski, D. M., Salit, I., Simor, A. E., Slutsky, A. S., Doyle, P. W., Krajden, M., Petric, M., Brunham, R. C., and McGeer, A. J. (2003) N. Engl. J. Med. 348, 1995-2005.

[5] Lee, N., Hui, D., Wu, A., Chan, P., Cameron, P., Joynt,G. M., Ahuja, A., Yung, M. Y., Leung, C. B., To, K. F., Lui, S. F., Szeto, C. C., Chung, S., and Sung, J. J. (2003) N. Engl. J. Med. 348, 1986-1994.

[6] Tsang, K. W., Ho, P. L., Ooi, G. C., Yee, W. K., Wang, T., Chan-Yeung, M., Lam, W. K., Seto, W. H., Yam, L. Y., Cheung, T. M., Wong, P. C., Lam, B., Ip, M. S., Chan, J., Yuen, K. Y., and Lai, K. N. (2003) N. Engl. J. Med. 348, 1977-1985.

[7] Hsueh, P. R., Chen, P. J., Hsiao, C. H., Yeh, S. H., Cheng, W. C., Wang, J. L., Chiang, B. L., Chang, S. C., Chang, F. Y., Wong, W. W., Kao, C. L., and Yang, P. C. (2004) Emerg. Infect. Dis. 10, 489-493.

[8] Lai, M. M. C., and Holmes, K. V. (2001) in: Fields Virology (Knipe, D. M. and Howley, P.M., Eds) Lippincott Williams and Wilkins, New York.

[9] Enjuanes, L., Brian, D., Cavanagh, D., Holmes, K., Lai, M. M. C., Laude, H., Masters, P., Rottier, P., Siddell, S. G. Spaan, W. G. M., Taguchi, F., and Talbot, P. (2000) in: Virus Taxonomy (van Regenmortal, M. H. V., Fauqet, C. M., Bishop, D. H. L., Carstens, E. B., Estes, M. K., Lemon, S. M., Mayo, M. A., McGeoch, D. J., Pringle, C. R., and Wickner, R. B., Eds) Academin Press, New York.

[10] Holmes, K. V. (2001) in: Fields Virology (Knipe, D. M. and Howley, P.M., Eds) Lippincott Williams and Wilkins, New York.

[11] Ziebuhr, J., Snijder, E. J., and Gorbalenya, A. E. (2000) J. Gen. Virol. 81, 853-879.

[12] Ho, Y. L, and Chang, Y. S. (2002) Phytomedicine 9, 419-424.

[13] Wu, X. Y., Qin, G. W., Cheung, K. K., and Cheng, K. F. (1997) Tetrahedron 53, 13323-13328.

[14] Qin, G. W., and Xu, R. S. (1998) Med. Res. Rev. 18, 375-382.

[15] Chend D. H. and Xie, J. X. (1984) Chin. Trad. Herb. Drugs 15, 6–8.

[16] Chang, C. N. (1985) in: H.M. Chang (Ed.), Adv. Chin. Med. Mater. Res. Int. Symp., World Sci., Singapore

[17] Hoessel, R., Leclerc, S., Endicott, J. A., Nobel, M. E. M., Lawrie, A., Tunnah, P., Leost, M., Damiens, E., Marie, D., Niederberger, E., Tang, W., Eisenbrand, G. and Meijer, L. (1999) Nat. Cell Biol. 1, 60–68.

[18] McGovern, S. L., and Shoichet, B. K. (2003) J. Med. Chem. 46, 2895-2907.

[19] Zhang, Y. W., Morita, I., Zhang, L., Shao, G.., Yao, X. S., and Murota, S. (2000) Planta Med.66, 119-123.

[20] Cabeza, M., Bratoeff, E., Heuze, I., Ramirez, E., Sanchez, M., and Flores, E. (2003) Proc. West Pharmacol. Soc. 46, 153-155.

[21] Hsueh, P. R., Hsiao, C. H., Yeh, S. H., Wang, W. K., Chen, P. J., Wang, J. T., Chang, S. C., Kao, C. L., Yang, P. C. (2003) Emerg. Infect. Dis. 9, 1163-1167.

[22] Lin, C. W., Tsai, C. H., Tsai, F. J., Chen, P. J., Lai, C. C., Wan, L., Chiu, H. H., and Lin, K. H. (2004) FEBS Letters, in press.

[23] Joubert, P., Pautigny, C., Madelaine, M. F., and Rasschaert, D. (2000) J. Gen. Virol. 81, 481-488.

[24] Cinatl, J., Morgenstern, B., Bauer, G., Chandra, P., Rabenau, H., and Doerr, H. W. (2003) Lancet 361, 2045-2046.

[25] Yamamoto, N., Yang, R., Yoshinaka, Y., Amari, S., Nakano, T., Cinatl, J., Rabenau, H., Doerr, H. W., Hunsmann, G., Otaka, A., Tamamura, H., Fujii, N., and Yamamoto, N. (2004) Biochem. Biophys. Res. Commun. 318, 719-725.

[26] He, R., Adonov, A., Traykova-Adonova, M., Cao, J., Cutts, T., Grudesky, E., Deschambaul, Y., Berry, J., Drebot, M., and Li, X. (2004) Biochem. Biophys. Res. Commun. 320, 1199-1203.

[27] Cinatl, J., Morgenstern, B., Bauer, G., Chandra, P., Rabenau, H., Doerr, H. W. (2003) Lancet 362, 293-294.

Figure Caption

Fig. 1.   SDS-PAGE (A) and Western blotting (B) of the purified SARS-CoV 3CL^{pro}. (A) The purified 3CL^{pro} recombinant protein at the 1 mg/ml was analyzed by 10% SDS-PAGE with Coomassie blue staining (lane2).   (B) After analyzing by SDS-PAGE, the 3CL^{pro} recombinant protein was electrophorectically transferred onto nitrocellulose paper.   The blot was probed with mouse anti-His tag antibodies, and developed with an alkaline phosphatase-conjugated secondary antibody and NBT/BCIP substrates.   Lane 1 was the molecular marker.   kDa, kilodaltons.

Fig. 2. Western blotting of the cis-cleavage of the 3CL^{pro} in Vero cells.   The lysates (100 μg) of the transfected with pcDNA3.1-3CL^{pro}/S-II/Luc were analyzed by 10% SDS-PAGE , then electrophorectically transferred onto nitrocellulose paper.   The blot was probed with mouse anti-luciferase monoclonal antibodies, and developed with an alkaline phosphatase-conjugated secondary antibody and NBT/BCIP substrates.   Lane 1, molecular markers; lane 2, un-transfected cells; lane 3 to 5, the transfected cells after the 1-, 2- and 3-week selection with 200 μg/ml G418.   kDa, kilodaltons.

Fig. 3.   Inhibition of the in vitro *trans*-cleavage of the 3CL^{pro} by the *Isatis Indigotica* root extract.   The extract of the *Isatis Indigotica* root was added into the mixture of the S-I/nsp7 fusion protein and the 3CL^{pro}, then incubated at room temperature for 3 h. The non-cleavage S-I/nsp7 fusion protein captured onto 96-well plates with anti-HSV mAb was detected using the S protein-HRP conjugate and ABTS/H_2O_2 substrates. The ELISA product was measured at A405 nm.   The relative inhibition of in vitro *trans*-cleavage activity was calculated as $1 - (A405_{no\ 3CL}{}^{pro} - A405_{3CL}{}^{pro}{}_{with\ inhibitor})/(A405_{no\ 3CL}{}^{pro} - A405_{3CL}{}^{pro})$.

Fig. 4.   Inhibition of the cell-based *cis*-cleavage of the 3CL^{pro} by the *Isatis Indigotica* root extract.   Vero cells carrying with pcDNA3.1-3CLpro/S-II/Luc were treated with the indicated concentration of the *Isatis Indigotica* root extract.   Equal amounts (100 μg) of cell lysates were used to determine the luciferase activity (LUC) using the dual Luciferase Reporter Assay System.   The relative inhibition of in vivo *cis*-cleavage activity was calculated as $1 - (LUC_{with\ inhibitor})/(LUC_{without\ inhibitor})$.

Fig. 5.   Inhibition of the *trans*-cleavage of the 3CL^{pro} by the compounds from *Isatis Indigotica* root.   The indicated compound was added into the mixture of the S-I/nsp7

fusion protein and the 3CL^{pro}, then incubated at room temperature for 3 h. The non-cleavage S-I/nsp7 fusion protein captured onto 96-well plates with anti-HSV mAb was detected using the S protein-HRP conjugate and ABTS/H_2O_2 substrates. The ELISA product was measured at A405 nm. The relative inhibition of in vitro *trans*-cleavage activity was calculated as $1 - (A405_{no\ 3CL^{pro}} - A405_{3CL^{pro}\ with\ inhibitor})/(A405_{no\ 3CL^{pro}} - A405_{3CL^{pro}})$.

Fig. 6. Inhibition of the *cis*-cleavage of the 3CL^{pro} by the compounds from *Isatis Indigotica* root. Vero cells carrying with pcDNA3.1-3CLpro/S-II/Luc were treated with the indicated compound. Equal amounts (100 μg) of cell lysates were used to determine the luciferase activity (LUC) using the dual Luciferase Reporter Assay System. The relative inhibition of in vivo *cis*-cleavage activity was calculated as $1 - (LUC_{with\ inhibitor})/(LUC_{without\ inhibitor})$.

Table. 1. The inhibitory effect on the in vitro *trans*-cleavage activity of the SARS-CoV 3CL^{pro} using ELISA

Table. 2. The inhibitory effect on the *cis*-cleavage activity of the SARS-CoV 3CL^{pro} in Vero cells using the luciferase assay
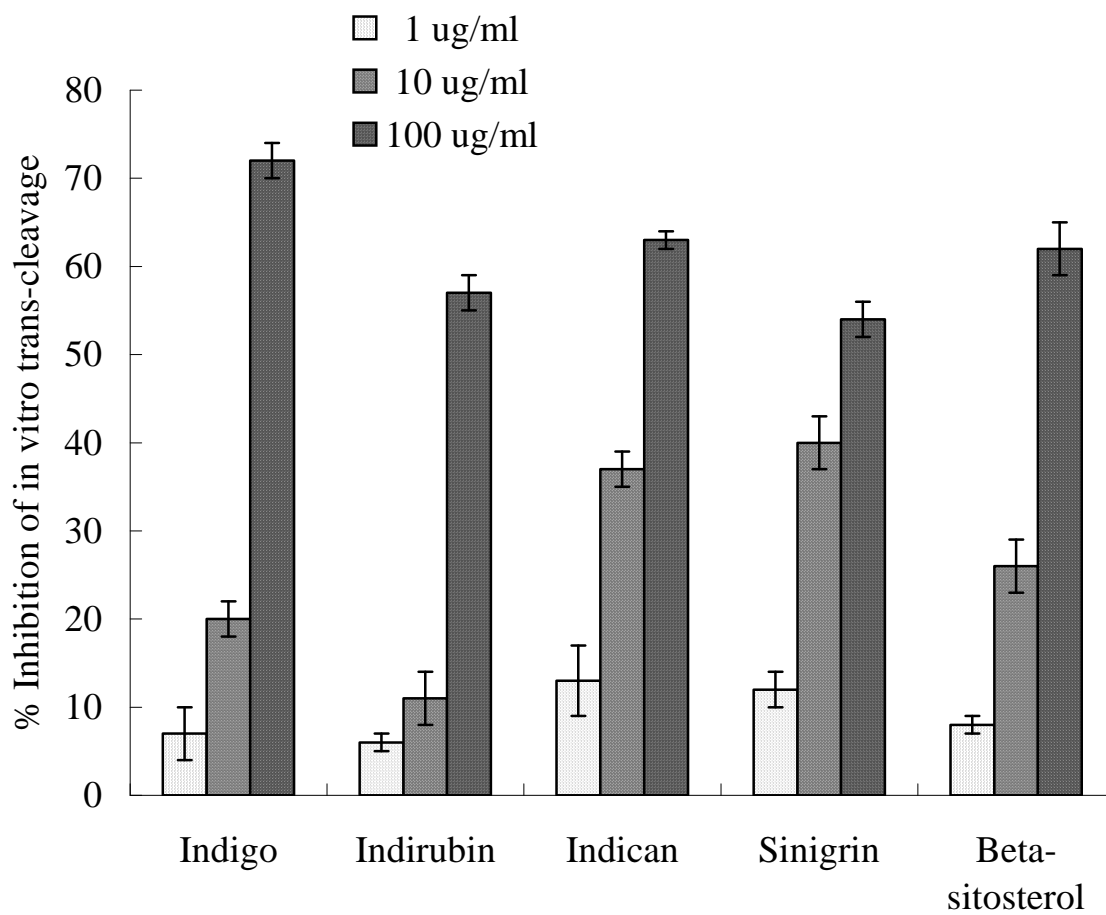
Fig. 1.

(A)
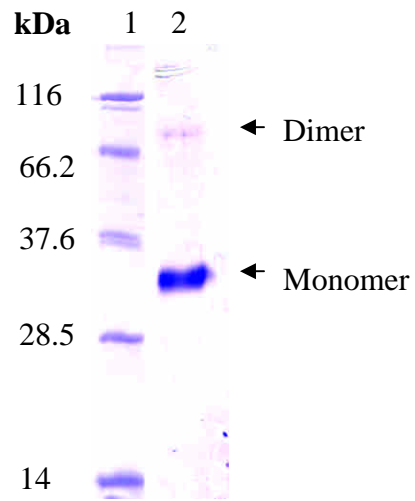
(B)
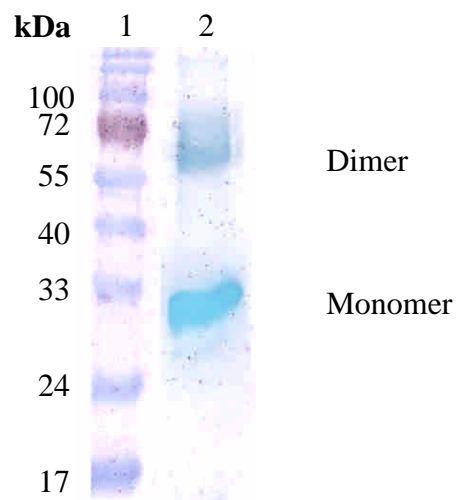
Fig. 2.
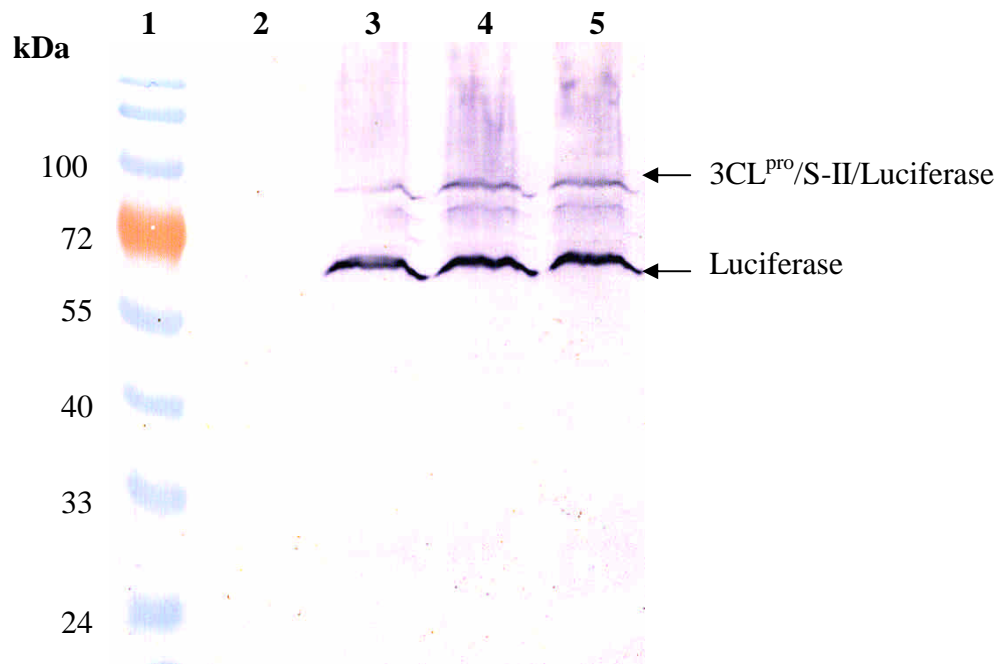
Fig. 3.
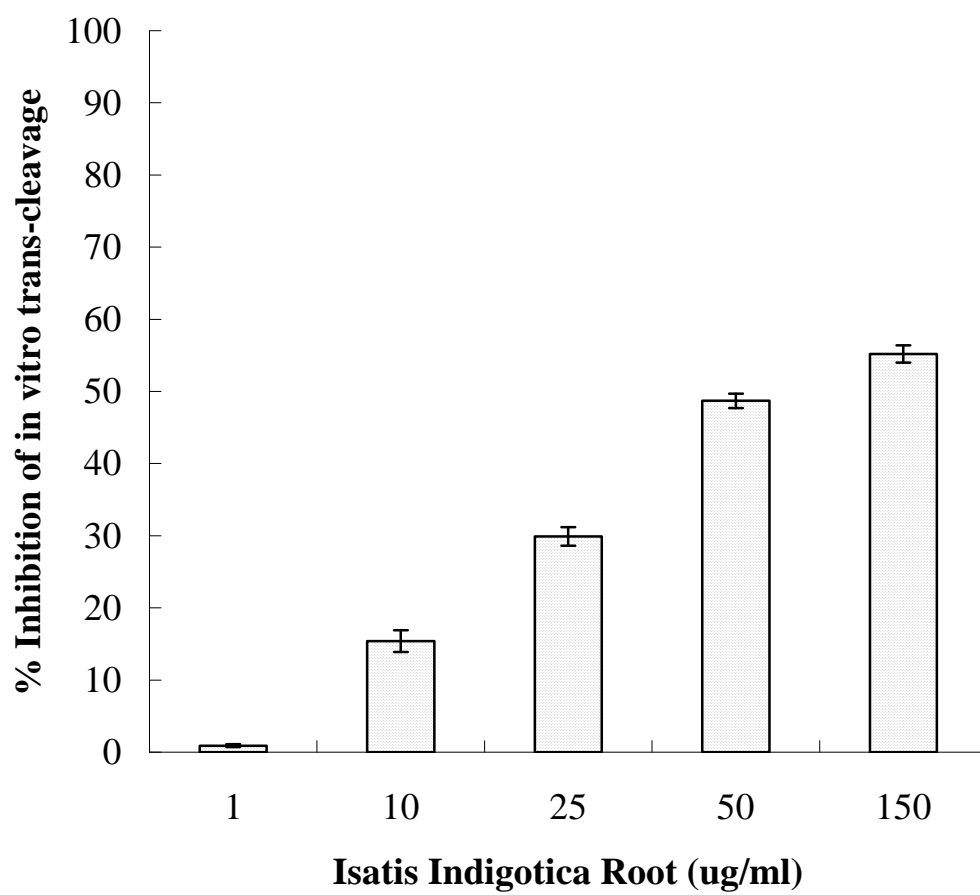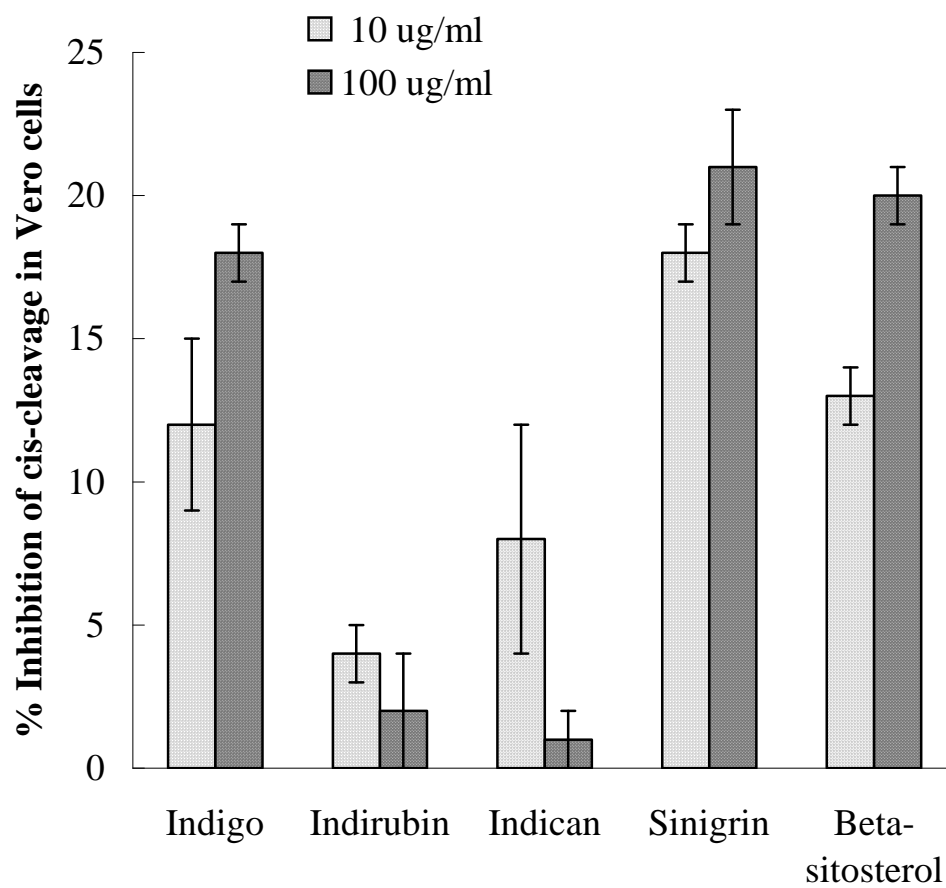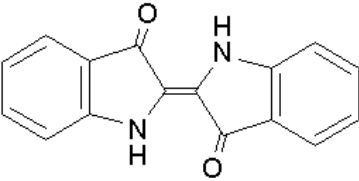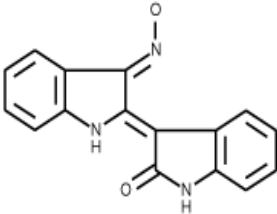
Fig. 4.
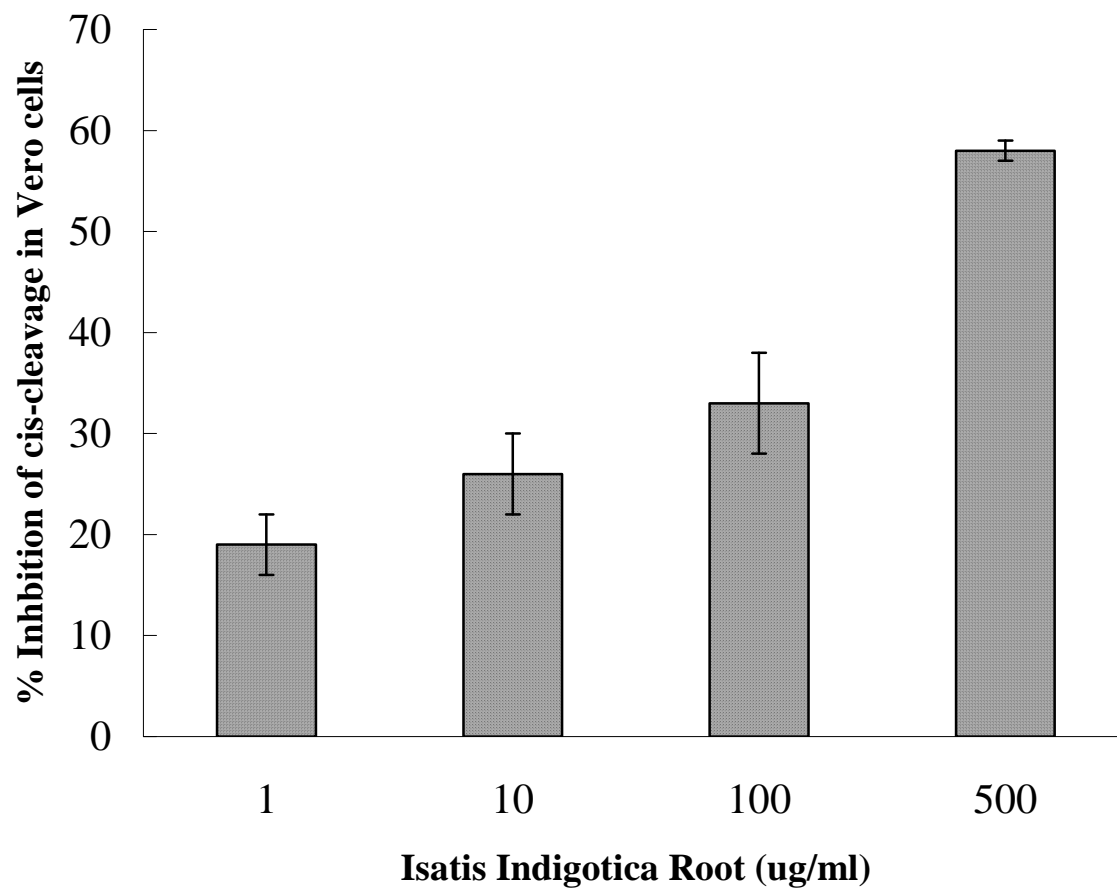
Fig. 5.
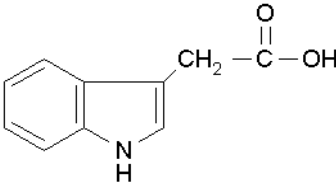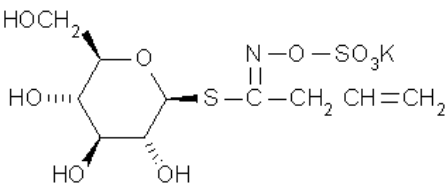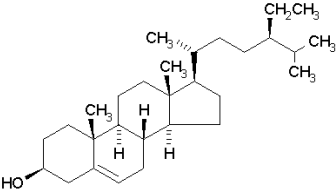
Fig. 6.

Table. 1

Compound	Structure	IC50 (μg/ml)
Isatis Indigotica **Root**		**80.3 ± 4.2**
Indigo		37.3 ± 8.1 (300 μM)
Indirubin		81.3 ± 5.2 (293 μM)
Indican		33.1 ± 1.2 (112 μM)
Sinigrin		50.3 ± 1.5 (121 μM)
Beta-sitosterol		47.8 ± 8.6 (115 μM)

Table. 2

Compound	IC50 (μ g/ml)	MTT metabolism [b] (% of control)
Isatis Indigotica Root	191.6 ± 8.2	93 ± 7
Indigo	> 1000	101 ± 8
Indirubin	ND[a]	122 ± 9 [c]
Indican	ND[a]	137 ± 2 [c]
Sinigrin	> 1000	124 ± 8 [c]
Beta-sitosterol	> 1000	101 ± 9

[a] No dose-dependent manner.
[b] Vero cells treated with 100 µg/ml of the indicated compound, except 500 µg/ml for the extract of Isatis Indigotic root.
[c] Stimulating cell growth.